

US-LARP Progress on LHC IR Upgrades

Tanaji Sen, John Johnstone, Nikolai Mokhov, FNAL, Batavia, IL 60510
Wolfram Fischer, Ramesh Gupta, BNL, Upton, NY

Ji Qiang LBNL, Berkeley, CA

Abstract

We review the progress on LHC IR upgrades made by the US-LARP collaboration since the last CARE meeting in November 2004. We introduce a new optics design with doublet focusing, and discuss energy deposition calculations with an open mid-plane dipole. We present the results of a beam-beam experiment at RHIC. This experiment was the first phase of a planned test of the wire compensation principle at RHIC.

I. Introduction

Increasing the luminosity in the LHC will require upgrades to the interaction regions (IRs) as well as to the injector chain. US-LARP is committing resources towards the development of the next generation magnets and to the optics design for the IR upgrade. Previous reports and reviews of LARP efforts on the IR upgrades can be found in references [1], [2] and elsewhere. Ideas for several alternative IR designs were proposed and some of their consequences on optics functions and energy deposition were discussed. Here we will present progress on the IR designs since the last CARE meeting in November 2004.

Mitigating the impact of the long-range interactions is one of the key motivations for exploring IR designs different from the baseline design. Wire based compensation of the long-range interactions has been proposed for the baseline design [3]. US-LARP has proposed to carry out a test of this wire

compensation in RHIC which has a layout similar to that of the LHC. Here we will also report on an experiment performed at RHIC to test the impact of a long-range interaction on the beams.

II. IR Designs

Design and construction of next generation IR magnets with Nb₃Sn technology constitutes the major portion of the US-LARP effort on IR design. The accelerator physics effort on IR design is mainly to provide guidance to the magnet builders. It is not intended to propose fully optimized optics designs that satisfy all known engineering and physics constraints. Due to the complex environment of the LHC IR magnets, beam optics by itself does not suffice to determine the aperture and gradient of these magnets. Energy deposition in the IR magnets is a key component in determining these parameters. The required field quality is another key input to the magnet designers. An IR design that meets most of the basic criteria can be useful for initial estimates of the required field quality. More careful evaluations of the field quality will be required as we progress towards the final design. Thus apertures, fields, field quality, demands on correction systems, energy deposition can all be estimated with preliminary IR designs. That is our purpose here.

In this report we will consider three different designs: the baseline design and two variants of the dipole first design. One of these variants is new with doublet focusing which produces elliptical beams at the IP. It has the

promise of higher luminosity but perhaps at the expense of enhanced beam-beam effects. We will also present energy deposition results with dipole first optics and the use of a novel open mid-plane dipole. It should be emphasized that the results shown here represent work in progress and much remains to be done.

II.A Optics of the IR Designs

The baseline design features quadrupoles built with NbTi superconductor. They are placed as close as possible to the IP and designed for $\beta^* = 0.50$ m. The promise of Nb₃Sn for the upgrade is that higher pole tip fields are achievable. This can be used to either (a) increase the gradient with the same physical aperture and decrease magnetic lengths – allowing the triplet magnets to move closer to the IP or (b) keep the gradient constant but increase the physical aperture. A previous study [4] had showed that option (b) was the superior path to higher luminosity.

In the designs to be presented here, we consider the inner triplet magnets to be at the fixed gradient of 200 T/m at top energy – the same as in the baseline optics. The matching section extends from the trim quadrupole QT13 on the left to the trim quadrupole QT13 on the right. We've used the LHC optics version 6.2. The optics constraints are the standard ones. Starting from the left, we match to the required β^* at the IP keeping α and dispersion and its slope zero at the IP. At the end of the section, the values of β , α , dispersion and its slope are matched. Taking into account both planes, this amounts to 16 matching constraints. We have not attempted to keep the phase advance the same as in the baseline optics. In the cases where we've developed solutions both at

injection and collision, we have kept the phase advance across the section constant. While we recognize that a complete optics design requires solutions at injection, through different stages of the squeeze and ending with the collision optics, we have mainly focused on the design at collision energy to demonstrate the feasibility of the design and the impact on luminosity.

We discuss the baseline design first. All positions and lengths of magnets are assumed to be unchanged. A design that reduced the β^* to 0.25m had been presented earlier [5]. A drawback in that design was that the gradient in one magnet exceeded 200 T/m. In the present design all gradients are at or under 200 T/m. Figure 1 shows the beta functions in the matching section.

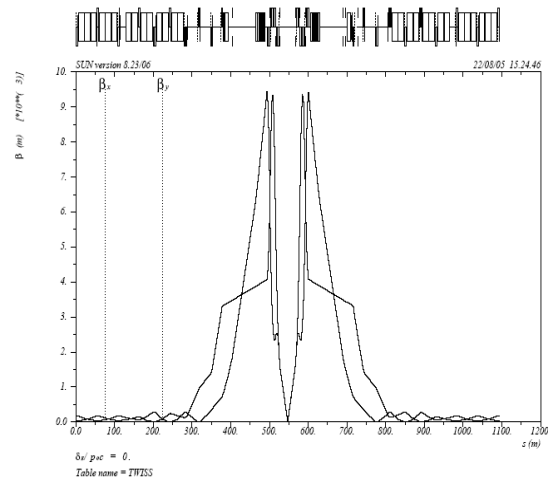


Figure 1: Beta functions in the baseline design with $\beta^* = 0.25$ m.

The maximum beta values occur in Q2b and Q3 and are twice the values with $\beta^* = 0.50$ m. Magnet coil apertures and pole tip fields can be extracted from this solution. We calculate the coil aperture as follows:

$$Aperture = 1.1(Beamsep + 2 \times Beamenv) + 2(Orbit + beampipe + Hechan + beamscre) \quad (1)$$

The factor 1.1 accounts for a 20% β beating, the beam separation (in units of s) is 10, the beam envelope is 9, orbit distortions total 8.6 mm including contributions from on-momentum errors (3mm), dispersion (4 mm), mechanical alignments (1.6 mm), the beam pipe thickness is 3 mm, the liquid He channel is 4.5 mm and the beam screen thickness is 1 mm. From the aperture and the gradient we calculate the pole tip field without assuming any additional margins. These are shown in Table 1 for the baseline optics.

| Quad | Gradient [T/m] | Aperture [mm] | Pole tip field [T] |
|------|----------------|---------------|--------------------|
| Q1 | 200. | 80.8 | 8.1 |
| Q2a | 200. | 100.2 | 10.0 |
| Q2b | 200. | 100.7 | 10.1 |
| Q3 | 200. | 101.0 | 10.1 |
| Q4 | 82. | 73.9 | 3.0 |
| Q5 | 67. | 61.4 | 2.1 |
| Q6 | 59. | 55.8 | 1.6 |
| Q7 | 199. | 45.8 | 4.6 |
| Q8 | 155. | 45.3 | 3.5 |
| Q9 | 155. | 45.9 | 3.6 |
| Q10 | 193. | 42.8 | 4.1 |
| QT11 | 56. | 43.4 | 1.2 |
| QT12 | 55. | 43.5 | 1.2 |
| QT13 | 40. | 43.4 | 0.9 |

Table 1: Gradients, apertures and pole tip fields for the baseline optics shown in Figure 1.

While the gradients are not exactly left right symmetric, the differences are less than 15%. Table 1 shows the maximum values. The realistic pole tip fields will likely be higher when margins are added. It is clear therefore that even with the baseline optics, Nb_3Sn technology will be required for the inner triplet

magnets whose pole tip fields exceed 9 T.

We now discuss the first of the two dipole first layouts. This is the same layout discussed in previous reports [6], [1], [2]. The separation dipoles D1 and D2 are placed right after the TAS absorber to separate the beams early and minimize the number of long-range interactions. Figure 2 shows the conceptual layout of the separation dipoles followed by the triplet focusing channel for both beams on both sides of the IP. The optics is anti-symmetric about the IP.

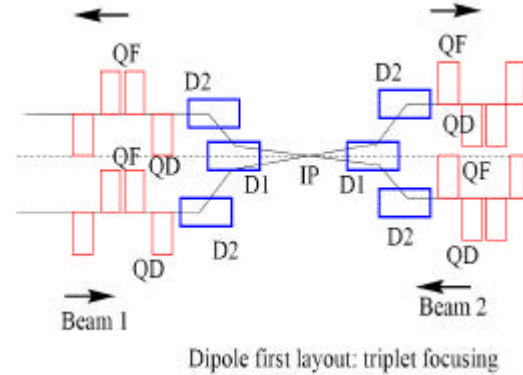


Figure 2: IR layout with dipoles first and triplet focusing. The focusing is anti-symmetric about the IP for each beam. The TAS and TAN absorbers are not shown.

Energy deposition in the magnets downstream of the dipoles is a major issue with this optics [1], [2]. In order to mitigate the power deposited in D2 and the triplet magnets, an additional absorber TAS2 has been introduced. Calculations with the open mid-plane dipole design for D1 show that an integrated field of 20 T-m before this absorber is necessary in order for most of the energetic particles to be deflected into the absorber. Therefore D1 originally 10m long is split into two pieces: D1A 1.5m long and D1B 8.5m long with the TAS2 absorber placed

between them. An additional absorber TAN, for neutral particles, is estimated to be 5m long and placed after D2. Any realistic optics design has to incorporate these absorber lengths from the outset. Table 2 shows the relevant lengths and distances for the triplet version of the dipole first optics. The first focusing element Q1 starts at 55.5m from the IP compared to 23 m from the IP in the baseline optics.

| | |
|------------------------|-----------|
| Length of TAS1 | 1.8 m |
| Distance of D1 from IP | 23 m |
| Length of D1A/D1B | 1.5/8.5 m |
| Length of TAS2 | 1.5 m |
| Length of TAN | 5 m |
| Distance of Q1 from IP | 55.5 m |
| Length of Q1/Q3 | 4.99 m |
| Length of Q2a/Q2b | 4.61 m |

Table 2: Relevant lengths up to the inner triplet in the triplet focusing version of the dipole first optics.

In order to make minimal changes to the insertion, the positions of the downstream magnets Q4 to QT13 have been kept at the same positions as in the baseline optics. This is strictly not necessary – the magnets Q4 to Q7 before the start of the dispersion suppressor could be placed differently. In future iterations we will make use of this flexibility. Figure 3 shows the beta functions across the matching section.

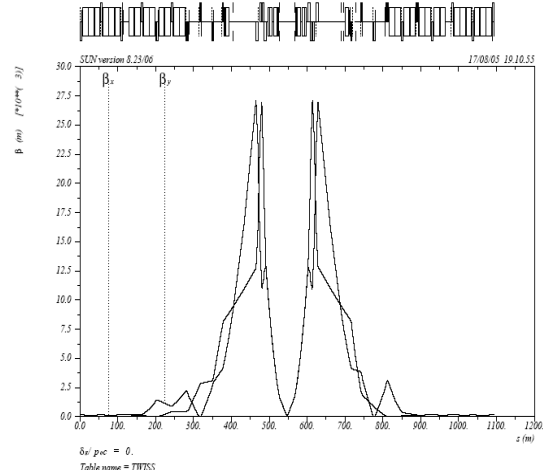


Figure 3: Beta functions across the matching section at collision in the triplet focusing version of the dipole first optics.

The peak beta functions are about 27 km in the triplet quadrupoles compared to about 9 km in the baseline optics for the same $\beta^*=0.25$ m. The optics is not left right symmetric beyond Q7. This can be improved with changes such as repositioning the Q4 to Q7 quadrupoles. Table 3 shows the important parameters that can be extracted from this solution: the apertures and the pole tip fields. Only one beam needs to be accommodated in each aperture and there is no need to include the beam separation factor in Equation (1) or the factor of 2 before the beam envelope term.

| Quad | Gradient [T/m] | Aperture [mm] | Pole tip field [T] |
|------|----------------|---------------|--------------------|
| Q1 | 200. | 94.8 | 9.5 |
| Q2a | 200. | 107.3 | 10.7 |
| Q2b | 200. | 107.1 | 10.7 |
| Q3 | 200. | 107.0 | 10.7 |
| Q4 | 112. | 74.5 | 4.2 |
| Q5 | 137. | 61.7 | 4.2 |
| Q6 | 80. | 57.9 | 2.3 |
| Q7 | 172. | 58.9 | 5.1 |
| Q8 | 196. | 47.9 | 4.7 |
| Q9 | 92. | 50.9 | 2.3 |

| | | | |
|------|------|------|-----|
| Q10 | 230. | 40.8 | 4.7 |
| QT11 | 170. | 40.6 | 3.5 |
| QT12 | 156. | 40.2 | 3.1 |
| QT13 | 160 | 40.1 | 3.2 |

Table 3: Gradients, coil apertures and pole tip fields for the triplet focusing version of the dipole first optics.

Compared to the apertures and pole tip fields seen in Table 1 for the baseline optics, the values for this optics are higher. Nb₃Sn magnets will be required even for the first quadrupole Q1 in the triplet in this optics.

Finally we discuss the doublet focusing optics for the insertion. Such focusing has conventionally been used in e⁺e⁻ colliders with 2 rings. We can explore the feasibility of doublets in the dipole first option where the focusing occurs in separate channels. We require symmetric focusing around the IP in order to have nearly equal beta functions in both planes upstream and downstream of the IP. The transverse beam sizes are unequal at the IP but they can still be matched between the beams provided each beam sees the same focusing sequence in the doublets. The crossing plane determines the polarity of the quadrupole Q1 nearest to the IP. We want to maximize the overlap between the beams. If the crossing plane is horizontal, then the horizontal beam size should be larger to increase the overlap. This implies that the nearest quadrupole Q1 should be vertically focusing – this argument assumes that β^{\max} in the two planes are nearly the same. Maximizing the overlap leads to an important advantage in luminosity as will be shortly seen. Figure 4 shows the layout with the doublet focusing.

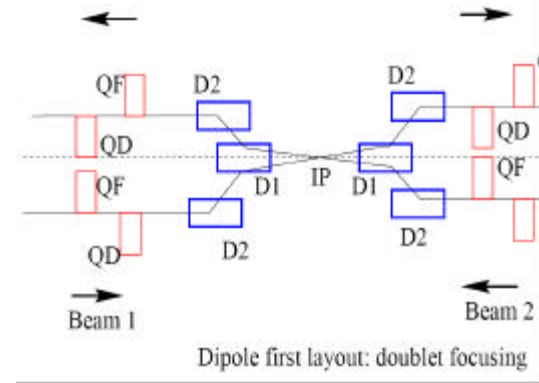


Figure 4: IR layout with dipoles first and doublet focusing. In contrast to the triplet focusing, the focusing is symmetric about the IP from Q1 to Q3 for each beam. On a given side of the IP, the quadrupole polarities are opposite for the two beams. This figure should be compared with Figure 2.

Unequal beam sizes imply that the head-on beam-beam tune shifts will also be different in the two planes. However with alternating crossing planes, this is easily resolved. At IP1 where the crossing plane is vertical the vertical head-on beam-beam tune shift is larger while at IP5 with a horizontal crossing plane, the horizontal head-on tune shift is larger resulting in equal head-on tune shifts. This requires that the quadrupole nearest to the IP for a given beam have the opposite polarities at IP1 and IP5.

Another benefit of the dipole focusing is that with fewer magnets it is cheaper than using triplets and also results in lower nonlinear fields on the beams.

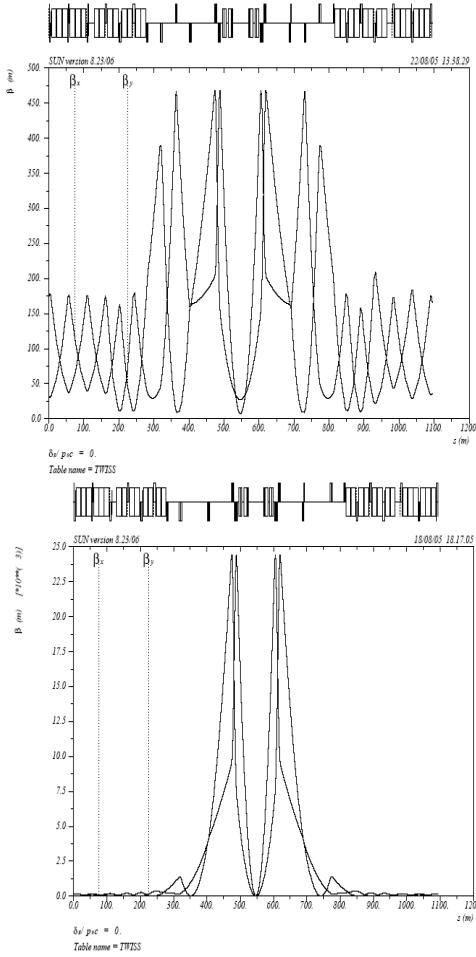


Figure 5: Matched optics at injection (top) and at collision (bottom) across the insertion for the doublet focusing version of the dipole first optics.

The solution that has been developed uses a doublet Q1 and Q2 with the same lengths and strengths. An additional trim quadrupole Q1Trim is required for matching purposes. The quadrupoles Q3, Q4 form another doublet. Figure 5 shows the matched optics at injection and collision. All quadrupoles from Q1 to Q6 are at different locations compared to the baseline optics. The insertion has to match to an anti-symmetric arc with respect to the IP. The insertion is symmetric about the IP up to Q3 but anti-symmetric from Q4 onwards. At collision the β^* values in the two planes are $\beta_x^* = 0.462$ m and $\beta_y^* = 0.135$ m

whose geometric mean is $\beta^* = 0.25$ m. For magnet designers, the important quantities are the apertures and the pole tip fields – these are shown in Table 4.

| Quad | Gradient [T/m] | Aperture [mm] | Pole tip field [T] |
|------|----------------|---------------|--------------------|
| Q1 | 198 | 103.6 | 10.3 |
| Q2 | 198 | 103.6 | 10.3 |
| Q1T | 125 | 96.9 | 6.1 |
| Q3 | 46 | 62.9 | 1.4 |
| Q4 | 50 | 61.5 | 1.5 |
| Q6 | 155 | 49.3 | 3.8 |
| Q7 | 31 | 44.2 | 0.7 |
| Q8 | 147 | 42.9 | 3.2 |
| Q9 | 205 | 41.3 | 4.2 |
| Q10 | 198 | 40.6 | 4.0 |
| QT11 | 98 | 40.2 | 2.0 |
| QT12 | 44 | 40 | 0.9 |
| QT13 | 108 | 40 | 2.2 |

Table 4: Gradients, coil apertures and pole tip fields for the doublet focusing version of the dipole first optics.

In both versions of the dipole first optics, coil apertures in excess of 100 mm will be required for the quadrupoles that are next to the separation dipoles. Even taking into account the space required for the coil and yoke assembly, there should be enough space between the two apertures given that the center to center distance between beams is 194 mm. However at larger apertures, magnet design issues such as Lorentz forces and stresses and cross talk between the two apertures impose an upper limit.

Consider now the impact on luminosity with elliptical beams at the IP. The beam separation is kept at 10σ with a crossing angle that scales inversely with the square root of β^* . Since β^* is larger in the crossing plane,

the required crossing angle with elliptical beams to achieve the same separation is smaller than with round beams by the factor

$$\mathbf{j}_E = \sqrt{\frac{\mathbf{b}_{R,E}^*}{\mathbf{b}_{E,E}^*}} \mathbf{j}_R = 0.74 \mathbf{j}_R \quad (2)$$

where the subscripts E and R refer to elliptical and round respectively. This directly increases the luminosity, a simple estimate of the change can be found from using the expression

$$\frac{L_E}{L_R} = \left[\frac{1 + (\mathbf{j}_R \mathbf{s}_s / \mathbf{s}_{x,R}^*)^2}{1 + (\mathbf{j}_R \mathbf{s}_s / \mathbf{s}_{x,R}^*)^2 (\mathbf{b}_{x,R}^* / \mathbf{b}_{x,E}^*)^2} \right]^{1/2} \quad (3)$$

This yields a factor of 1.38 but does not take into account the hourglass effect which is important in the vertical plane where the β^* is comparable to the bunch length of 7.5cm. A more complete luminosity calculation taking into account the overlap in both planes yields

$$\frac{L_E}{L_R} = 1.33 \quad (4)$$

This luminosity increase is a major advantage of using elliptical beams with crossing angles.

The head-on beam-beam tune shift with alternating crossing planes is the same as with round beams. The long-range beam-beam tune shifts also need to be examined. Here round beams have an advantage. With alternating crossing planes, the negative (zero-amplitude) horizontal tune shifts at large amplitudes beyond $4s$ at the IP with horizontal crossing are almost exactly cancelled by the positive horizontal tune shifts at the IP with a vertical crossing plane. There is a similar cancellation of the vertical tune shifts. However with elliptical beams, the vertical tune shifts are large and positive at the IR with horizontal crossing while at the other IR with

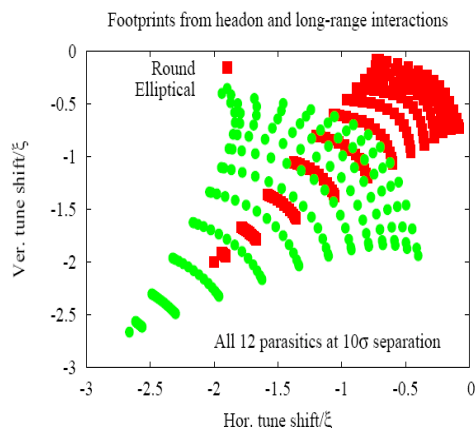


Figure 6: Tune footprint to 6σ with head-on and long-range interactions from IP1 and IP5 (calculated analytically) for the two versions of the dipole first optics. There are 12 parasitics per IR, 24 in all from IR1 and IR5.

vertical crossing, the vertical tune shifts are negative but not nearly as large. Therefore the cancellation is not nearly as good. As a consequence the long-range beam-beam tune shifts at all amplitudes are larger. In the dipole first optics, there are 6 long-range interactions on either side of the IP before the beams are in separate channels. The tune footprints with all 24 long-range interactions from IR1 and IR5 have been calculated analytically with the expressions in Reference [7] and are shown in Figure 6. As an example, the zero amplitude tune shifts with round beams are 2ξ (the beam-beam parameter) while with the elliptical beams used in this design, the corresponding tune shift is nearly 2.7ξ . It is possible that exploring other layouts, such as inclined plane crossings, may mitigate this effect but at the expense of luminosity. It remains true nonetheless that the long-range beam-beam effects are more of a concern with the elliptical beams and needs to be resolved. One possibility is to use wire-based compensation [3].

Finally we consider the chromaticity of the insertion in the three designs considered here. We use exact expressions for the chromaticity of thick quadrupoles. We show the chromaticity of the insertion and the inner magnets for each design in Table 5.

| Optics | Insertion Q_x'/Q_y' | Inner Magnets Q_x'/Q_y' |
|-------------------------|--------------------------|---------------------------------|
| Quads first | -48/-48 | -44/-44 |
| Dipoles first: triplets | -99/-96 | -82/-82 |
| Dipoles first: doublets | -105/-121 | -103/-112 |

Table 5: Chromaticity of an insertion and of the inner magnets for the three optics designs.

This table shows the chromaticity of a single IR. Clearly the inner triplet and inner doublet dominate the chromaticity. If we include both IR1 and IR5 then (a) chromaticity of dipoles first with triplets is 99 units larger per plane than the design with quadrupoles first, (b) chromaticity of dipoles first with doublets is 31 units larger per plane than dipoles first with triplets. The reason for (a) is simply the much larger beta functions in the inner magnets with the dipole first optics. A closer look at the chromaticity contributions from individual quadrupoles shows the reason for (b). With anti-symmetric optics upstream and downstream quadrupoles have opposite chromaticities and tend to cancel. With symmetric optics: upstream and downstream quadrupoles have the same sign of chromaticities. This can be seen in Figure 7 where the horizontal chromaticity contributions from the quadrupoles are plotted for the three designs.

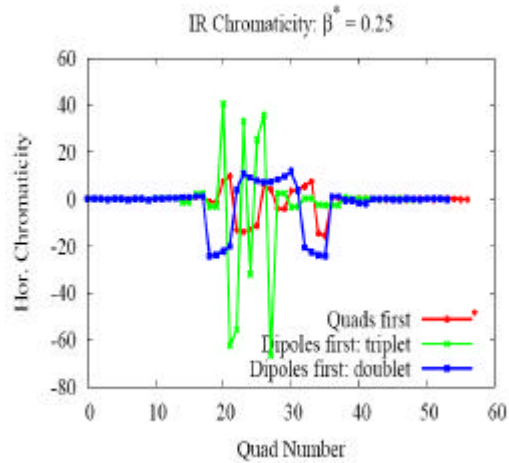


Figure 7: Horizontal chromaticity contributions from individual quadrupoles in the IR for the 3 designs. With the anti-symmetric optics (red and green), the chromaticities upstream and downstream of the IP have opposite signs. For the symmetric optics (blue) the chromaticities upstream and downstream have the same signs.

It remains to be checked whether the linear and nonlinear chromaticities of the different IR designs can be adequately corrected with the available LHC chromaticity sextupoles.

II.B Energy Deposition

Energy deposited by particles affect accelerator operation in at least four distinct ways. Quench stability is determined by the peak power density. The dynamic heat loads on the cryogenics is determined by the amount of power dissipated in the magnets. Hands-on maintenance is determined by the residual dose rates. Finally the lifetime of components is determined by the peak radiation dose and the lifetime limits which vary for different materials.

For some time now it has been recognized that energy deposition and the spray of particles from the IP will be the major issues for a ten-fold luminosity upgrade. At a luminosity of 10^{35} cm^{-2}

sec^{-1} , the debris power will be 9kW. All of this debris power will be directed towards the IR magnets which have to be well protected. In the baseline design with quadrupoles first, 1.6 kW will be absorbed within the triplet. At these dosages, the lifetimes of conventional insulators used for the magnet ends extends only to several months.

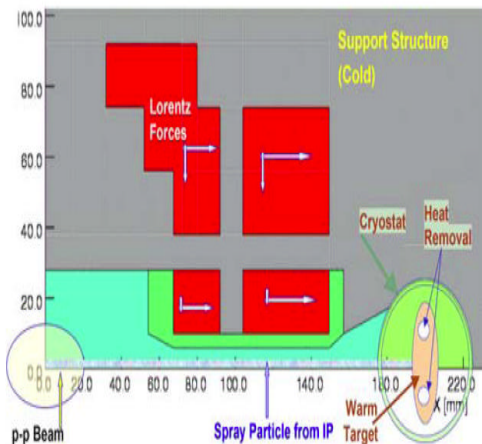


Figure 8: Sketch of the open mid-plane dipole design with no coils in the mid-plane. The warm targets are Tungsten rods at liquid N_2 temperature.

A significant part of the US-LARP magnet effort is therefore focused on developing more radiation hard materials. The energy deposition problem is more severe in the dipole first layout – so some effort has been invested in developing a dipole design that can withstand the expected radiation [8]. An open mid-plane design was developed with no coils in the mid-plane, seen in Figure 8. A major part of the particle spray is transported to Tungsten rods at liquid nitrogen temperatures, placed outside the coils. Several technical challenges were addressed including obtaining good field quality even with a large gap between the coils and supporting the coils against the large Lorentz forces on them. Energy

deposition analysis with this dipole split into D1A and D1B (as mentioned earlier) showed that TAS protects D1A quite well. Higher energy charged particles that are not absorbed in TAS and those generated in D1A are absorbed efficiently in TAS2. The minimum integrated field required before TAS2 is 20 T-m. The calculations show that the peak power density in the superconducting coils $\sim 0.4\text{mW/g}$, about a factor of three below the quench limit. The dynamic heat load to D1 is drastically reduced with this design. The estimated lifetime based on displacements per atom is ~ 10 years. These initial calculations suggest that if this design was to prove realistic, then it might survive the radiation environment long enough to be useful. Due to budgetary constraints, the US-LARP magnet program has decided to focus entirely on building the next generation quadrupoles and to postpone further work on the dipoles for the LHC IR.

III Beam-beam phenomena

RHIC has the same geometrical layout as the LHC with two rings, called yellow and blue. The optics of RHIC corresponds to the dipoles first layout with triplet focusing discussed above. Within the common IR where the beams share the same beam pipe, there can be no more than two parasitic interaction at the current bunch spacing in RHIC. Due to adverse phase advances, only a single parasitic can potentially be corrected in RHIC. In order for RHIC to be a practical test bed of the wire compensation principle, we first have to demonstrate that this single parasitic interaction has an observable effect to be compensated.

In April 2005 an experiment was performed at the injection energy of 24.3 GeV with a single proton bunch in each beam. This choice of energy allowed several experiments with both bunches at full intensity. The experiment consisted of changing the vertical separation between the beams at one parasitic interaction while the beam losses were observed. The separation at the diametrically opposite parasitic in the ring was kept constant at $\sim 10s$. The experiment was done four times with four different tunes. For the first three tunes only the blue beam suffered losses as the separation was reduced below a certain value. The yellow beam suffered very few losses at these tunes. In the fourth case, the tunes of the two beams were chosen to be symmetric about the diagonal. In this case, as seen in Figure 9, there were losses in both beams at separations smaller than $7s$. This experiment showed that there is indeed an effect to compensate, at least at injection energy, but the phenomena is very tune dependent.

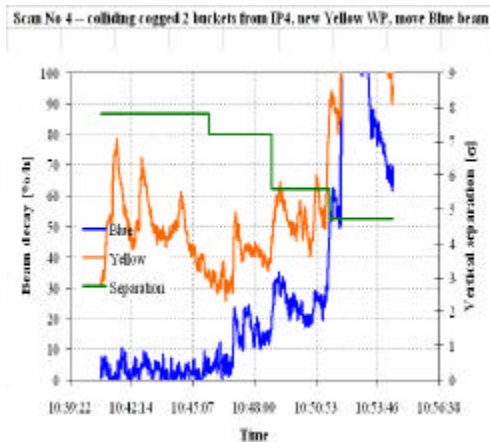


Figure 9: Losses in the blue beam, yellow beam (in red) and the beam separation (in green) for the fourth tune. There was a sharp increase in losses in both beams as the separation dropped below $7s$.

In the next phase of this program the experiment will be repeated at collision energy. At this energy the phase advance between the parasitic location and the possible location of the wire is 6° , perhaps still small enough for the wire compensation to work.

Over the next year, it is planned to build and install two wires in the two rings of RHIC, downstream of Q3 for each beam in IR6. Figure 10 shows the schematic layout on one side of IR6. The single parasitic occurs before the separation dipole DX.

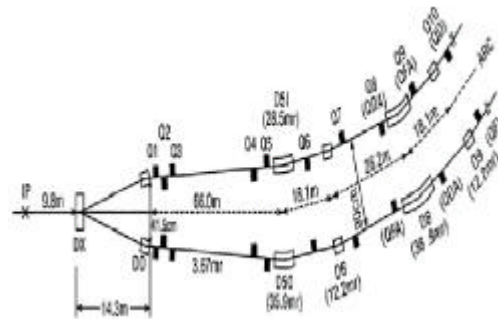


Figure 10: Sketch of IR6 in RHIC where the wire compensator will be placed, roughly 41m from the IP.

The first tests with these wires will likely take place during 2007. We also aim to test robustness of compensation with respect to current ripple, alignment errors etc.

A separate effort has been the development of a strong-strong beam-beam simulation PIC style code Beambeam3D [8]. In the past it has been used to study the emittance growth when one beam is swept around the other, as would be done for the luminosity monitor designed and built at LBNL. Recently more physics has been added to this simulation code including crossing angles, and long-range interactions.

Numerical noise remains a difficult issue to resolve – the calculated growth rate depends on the number of macro-particles M . Studies to extract asymptotic growth rates in M continue. Very recently the emittance growth with round and elliptical beams at the IPs has been studied.

IV Magnets

We will discuss the US-LARP magnet program very briefly. At the LARP collaboration meeting in April 2005 it was decided to concentrate the effort on the quadrupole program and postpone the dipole program. The major goals that were set were (a) demonstrate by 2009 that Nb_3Sn magnets are a viable choice for the upgrade and (b) demonstrate that these magnets with the required aperture, field, and length can be built with reproducible performance. A plan to realize these goals has been defined. Over the near term the plan is to build short quadrupoles (1 m long) with 90 mm aperture and 200 T/m gradients. These will be followed by longer quadrupoles (4 m long) with other parameters the same. Higher gradient (250 T/m), short (1 m long) quadrupoles will also be built. Other aspects of the magnet program include supporting R&D to build magnets with different geometries, test the capability to reach higher fields, develop radiation hard insulators etc. See reference [10] for details.

V Summary

We have discussed three optics designs for the upgrade: the baseline with quadrupoles first, dipoles first with triplet focusing, and dipoles first with doublet focusing. All three optics require magnets with apertures larger than 100 mm and pole tip fields greater than 10 T.

This implies that only Nb_3Sn magnets will suffice to realize the optics under the assumptions made here. The doublet focusing optics we discussed is new and has features both positive and negative. It creates elliptical beams at the IP. The resulting luminosity is about 33% greater than that obtained with round beams for the same effective β^* . This is partly due to the fact that the required crossing angle to achieve the same beam separation is smaller. The nonlinearities seen by the beams are smaller because of the smaller transverse orbit excursion and fewer magnets at high fields. On the negative side, the long-range beam-beam tune shifts are larger compared to round beams and the IR chromaticity with the use of doublets symmetric about the IP is larger than with asymmetric optics.

We mention here that other options were discussed at this Arcidosso workshop. These included moving magnets closer to the IP and installing a dipole magnet close to the detectors to start the beam separation as early as possible [11]. If realistic, these possibilities could be incorporated into the optics discussed here. Immediate benefits would be to reduce the requirements on aperture and pole tip fields.

Energy deposition studies with the open mid-plane dipole design showed that the severe radiation issues in the dipole first optics can be mitigated. This reinforces again the importance of including energy deposition early on in the designs of IR optics and magnets.

Beam-beam phenomena are also an important part of the IR upgrade studies. Test of the wire compensation principle is a new LARP program. The design of the wire compensators has begun and first tests of the wire compensation are planned for 2007.

Acknowledgements

We thank O. Bruning, J.P. Koutchouk, S. Peggs, F. Ruggiero, G.L. Sabbi, F. Zimmermann and A. Zlobin for valuable insights and useful discussions.

References

- [1] J. Strait et al, Proceedings of PAC 2003, page 42
- [2] J. Strait, N. Mokhov and T. Sen, CARE-HHH 2004 Proceedings
- [3] J.P. Koutchouk, LHC Project Note 223 (2000)
- [4] T. Sen et al, Proceedings of PAC 2001, page 3421
- [5] T. Sen et al, Proceedings of EPAC 2002, page 271
- [6] O. Bruning et al, LHC Project Report 626 (2002)
- [7] T. Sen et al, Phys, Rev, Spec. Top. AB, 7, 041001 (2004)
- [8] R. Gupta et al. Proceedings of PAC 2005, page 3055
- [9] J. Qiang et al, Phys, Rev, Spec. Top. AB, 5, 104402 (2002)
- [10] LARP R&D document
http://uslarp.lbl.gov/workshops/051102/files/RandD_v1c.pdf
- [11] J.P. Koutchouk, this workshop